Struct Multidisc Optim
DOI 10.1007/s00158-005-0573-6

INDUSTRIAL APPLICATIONS

László Gyulai · Szilárd Szabó · D. J. De Kock · J. A. Snyman

Optimal adjustment of the number of air changes of a smelter pot room by using mathematical optimisation

Received: 4 April 2005 / Revised manuscript received: 1 August 2005

Abstract The only large-scale, cost-effective way to exhaust contaminated air from the furnace pot room of an industrial plant is through natural ventilation. The effectiveness of the ventilation depends, amongst others, on the openings of the windows through which the air is allowed to enter and exit the workshop. The ventilation is also directly influenced by the prevailing weather outside the building. An appropriate measure that characterises the ventilation within the workshop is the number of air changes per hour, and ideally, it should be close to a prescribed value for all weather conditions. This requirement can be met by the appropriate adjustment of the opening angles of the inlet and outlet window slats. This paper reports on the feasibility of using mathematical optimisation to determine the ideal window slat angles for different prevailing wind conditions. The proposed optimisation methodology employs computational fluid dynamics software (FLUENT), coupled to a computationally economic optimisation algorithm (Dynamic-Q), to determine the optimal slat angles. Results of the successful application of the proposed optimisation procedure to an example problem of a large-scale aluminium smelter pot room are presented.

Keywords Successive approximation methods · Dynamic-Q optimisation algorithm · CFD simulations · Smelter pot room · Number of air changes

1 Introduction

In large-scale industrial workshops polluting gases and dust particles that cannot be extracted locally by exhaust fans are generated. Moreover, machines produce heat. Using natural ventilation is the only cost-effective way to decrease the temperature and the concentration of pollutant gases. Design methods for such large workshops have been known since the study of Baturin (1959). The design process is based on global parameters and considers a single representative weather condition. The design objective is to ensure sufficient natural ventilation (which is the result of unequal inner and outer temperatures) by well-placed and well-arranged windows. The number of air changes per hour, L, characterises the ventilation. This quantity is defined as the amount of air introduced per hour divided by the volume of the room of interest. The expected or required number of air changes, L_0, can easily be calculated if the limit on pollution concentration and the amount of pollutants present are taken into consideration similar to the study of Menyhárt (1977). Sufficient fresh air must be provided to reach a lower pollutant concentration. The ideally required number of air changes is, of course, dependent on the weather and climatic conditions. Thus, for fixed workshop ventilation settings, the actual number of air changes per hour, L, for different weather conditions, may seriously differ from the corresponding ideally prescribed number of air changes per hour, L_0. The free cross-sections of the windows can be changed by adjusting the opening angles of the windows. Thus, by appropriately adjusting these angles for different weather conditions, the corresponding ideal number of air changes may be approached.

The goal of this study is to develop a methodology by means of which it will be possible to determine the appropriate opening angles, for different prevailing weather conditions, that will ensure that the optimal required number of air changes are achieved. Until recently, there was no suitable and effective method to do this. In the present paper a method that couples a mathematical optimisation method (Dynamic-Q algorithm) and numerical simulation [Computational Fluid Dynamics (CFD)] is presented to solve the above problems. By using this method, it is possible to determine, for different weather conditions, suitable opening angles for the windows that will provide good ventilation. The method successfully minimises the difference between the actual and the ideally required number of air changes.

A much abbreviated version of the paper was read at the WCSMO6 ISSMO Congress in Rio de Janeiro, May 2005

László Gyulai (✉) · Szilárd Szabó
Department of Fluid and Heat Engineering,
University of Miskolc, Miskolc, Hungary
e-mail: aramgyl@uni-miskolc.hu

D. J. De Kock · J. A. Snyman
Department of Mechanical and Aeronautical Engineering,
University of Pretoria, Pretoria, South Africa

The proposed method is demonstrated by its application to an aluminium smelter pot room, for different prevailing wind velocities.

2 Specification of physical problem

The proposed methodology is applied to the aluminium smelter pot room situated in Inota, Hungary, which is representative of a plant where serious ventilation problems occur. Figure 1 shows the cross-sectional elevation of a big [440/40/17 m (length/width/height)] smelter pot room. In the smelter hall 176 electrolyser smelter pots are in operation. The heat loss causes high temperatures in the workshop. The inner and outer temperature difference results in a pressure difference, which causes fresh air to enter the pot room through the middle and bottom windows, as indicated in Fig. 1. The introduced fresh air dilutes the polluted air of the workshop. The quantity of the evolved gases is considered negligible compared to the quantity of fresh air introduced. In general, if the mixed gases exit the workshop through the roof windows at a rate of q_m kg/s, then q_m is also equal to the net rate at which fresh air enters through the windows. The ventilation of a pot room of volume V is characterised by the number of air changes per hour L, the definition of which is given by Menyhárt (1977) in the following form:

$$L\left[\frac{1}{\mathrm{h}}\right] = \frac{q_\mathrm{m}\left[\frac{\mathrm{kg}}{\mathrm{s}}\right] \cdot 3600\left[\frac{\mathrm{s}}{\mathrm{h}}\right]}{\rho\left[\frac{\mathrm{kg}}{\mathrm{m}^3}\right] \cdot V\left[\mathrm{m}^3\right]}, \tag{1}$$

where ρ is the mean density of air in the pot room. A sufficient number of air changes is necessary for primarily cooling the smelter pots, and secondly, for diluting the dust particles as well as the pollutant gases which evolve due to smelting, and thirdly, for evacuating them from the workshop. The definition of the air rinsing rate $q_{\mathrm{m},0}$, which allows for sufficient ventilation, and the form of L_0 are respectively given by

$$q_{\mathrm{m},0}\left[\frac{\mathrm{kg}}{\mathrm{s}}\right] = \rho\left[\frac{\mathrm{kg}}{\mathrm{m}^3}\right] \cdot \frac{q_{\mathrm{m,p}}[\mathrm{kg/h}] \cdot 10^{-6}[\mathrm{mg/kg}]}{k_\mathrm{a}[\mathrm{mg/m^3}] - k_\mathrm{out}[\mathrm{mg/m^3}]}, \tag{2}$$

$$L_0\left[\frac{1}{\mathrm{h}}\right] = \frac{q_{\mathrm{m},0}\left[\frac{\mathrm{kg}}{\mathrm{s}}\right] \cdot 3600\left[\frac{\mathrm{s}}{\mathrm{h}}\right]}{\rho\left[\frac{\mathrm{kg}}{\mathrm{m}^3}\right] \cdot V\left[\mathrm{m}^3\right]}, \tag{3}$$

where $q_{\mathrm{m,p}}$ (kg/h) is the rate at which pollutants evolve, k_a (mg/m^3) is the allowable pollution concentration and k_out (mg/m^3) is the ambient outside pollutant concentration.

From pollution rate considerations, the designer of the building has determined that the sufficient and adequate number of air changes per hour is L_0=30/h. For a couple of representative operating conditions, the actual number of air changes was measured by Szabó and Schifter (2000), and, for these conditions, they observed values close to that planned for, namely, L=27/h to 28/h. However, the weather conditions (i.e. the prevailing temperature, and magnitude and direction of the wind velocity) and the relative positioning and size of the surrounding buildings, as well as the local characteristic wind profile, have significant effects on the ventilation of the workshop. Therefore, in practice, the actual number of air changes L can significantly differ from the ideally prescribed number L_0 if the windows are kept opened at fixed angles, without allowance for changes in the weather conditions. In some cases, the L value may be less than that required (i.e. $L < L_0$), and, in other cases, especially if strong side winds occur, the value will be much higher than is necessary (i.e. $L > L_0$).

In the case of a low value of L, the ventilation will be inadequate, resulting in an increase in working zone temperature and pollution concentration. In case of a too high value of L, the working zone becomes too cool, and this results in strong blasts that gather and carry more and heavier polluting dust particles. It is therefore advisable to keep the number of air changes as near as possible to its prescribed designed-for value of L_0=30/h. This requirement can be ensured by the appropriate opening or closing of the side middle windows.

The window angles of each of the four rows of middle windows, two rows on each side of the workshop (see Fig. 1), are respectively indicated by x_1, x_2, x_3, x_4. It is required that, depending on the weather, these angles be separately adjusted to achieve the ideal number of air changes per hour. One

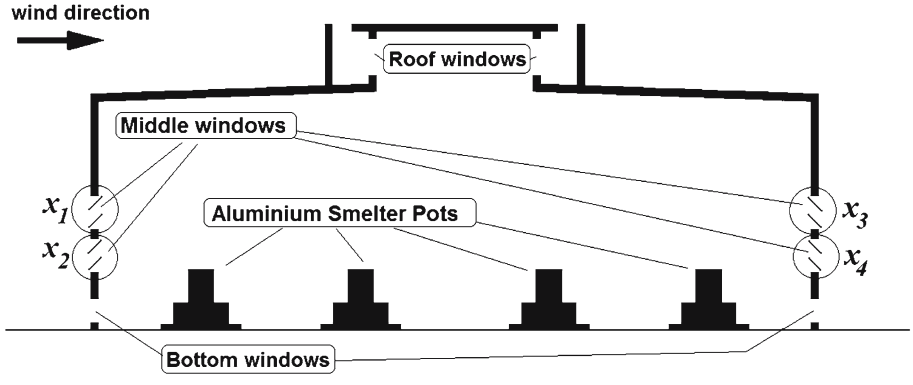

Fig. 1 Cross-sectional view of the smelter pot room

way, and that proposed here, of determining suitable opening angles of the windows is through the use of mathematical optimisation. In the optimisation approach proposed in this study, the objective function is taken as the absolute value of the difference between the required value of L_0 (taken here as L_0=30/h), and the actual number of air changes L, i.e. $|L-L_0|$. This objective function is to be minimised with respect to the four different window angles, which are taken as the respective optimisation or design variables x_1, x_2, x_3, x_4.

The whole optimisation process consists of two interacting parts. The first part is a frame program, which includes the optimisation code, and the second part is a CFD simulation program, which computes the ventilation number to be used in the objective function. Before detailing the application of the proposed optimisation methodology, it is necessary to review the basic theory of each part.

3 Mathematical optimisation algorithm

In principle, any appropriate computationally economic mathematical optimisation algorithm may be used to perform the optimisation. It should be economic, in terms of the number of iterations required for convergence, because of the computational cost associated with the simulations on which the optimisation is to be based. In this study, the method of choice is the relatively new Dynamic-Q algorithm, first introduced by Snyman et al. (1994) and very recently refined by Snyman and Hay (2002) and coded in FORTRAN. Apart from the fact that the authors are familiar with, and confident in the use of, this method, the algorithm was chosen for the following two reasons. First of all, Snyman and Hay (2002) thoroughly tested the method on a standard set of smooth test problems, compared its performance with that of the well-established Sequential Quadratic Programming (SQP) method and found its performance to be competitive, if not superior, to that of the SQP method. Secondly, this algorithm has already extensively and successfully been applied to computationally expensive simulation-based optimisation problems, where the objective function behaviour is not necessarily smooth due to numerical noise and where multiple local minima may also occur, as is expected in the current case. Some examples of the latter application of Dynamic-Q to simulation-based optimisation are the air pollution minimisation CFD study of Craig et al. (1999), the work on heat sink mass minimisation of Visser and De Kock (2002), as well as the very recent work of Els and Uys (2003) on vehicle suspension system design, and that of Hay and Snyman (2005) on the design of tendon-driven manipulators.

Although the Dynamic-Q method and its application are, as indicated above, well documented in the recent literature (refer also to the book by Snyman (2005)), it is nevertheless necessary to assist the reader here by presenting a brief outline of the method. The method involves the application of a dynamic trajectory method for unconstrained optimisation, described by Snyman (1982, 1992), and was adapted to handle constrained problems through appropriate penalty function formulations (Snyman et al., 1992). This Dynamic method is applied to successive approximate Quadratic sub-problems of the original problem. The successive sub-problems are constructed from sampling, at relative high computational expense, the behaviour of the constraint functions and/or objective function at successive approximate solution points in the design space. The sub-problems, which are analytically simple, are solved quickly and reliably using the adapted dynamic trajectory method, the latest version of which is described by Snyman (2000). With reference to the current study, the use of approximate sub-problems limits the number of simulations required for the solution of the original optimisation problem. A rough outline of the Dynamic-Q methodology now follows.

Consider the typical and general inequality constrained optimisation problem of the following form:

$$\text{Minimise } f(\boldsymbol{x}), \quad \boldsymbol{x} \in R^n \tag{4}$$

subject to the following inequality constraints

$$g_j(\boldsymbol{x}) \leq 0, \qquad j = 1, 2, ..., m \tag{5}$$

and equality constraints

$$h_k(\boldsymbol{x}) = 0, \qquad k = 1, 2, ..., r. \tag{6}$$

Usually an initial trial design $\boldsymbol{x}^{(0)}$ is available, and the solution to the above problem is denoted by $\boldsymbol{x}^*$.The penalty function referred to above is defined by

$$p(\boldsymbol{x}) = f(\boldsymbol{x}) + \sum_{j=1}^{m} \alpha_j g_j^2(\boldsymbol{x}) + \sum_{k=1}^{r} \beta_k h_k^2(\boldsymbol{x}), \tag{7}$$

where

$$\alpha_j = \begin{cases} 0 & \text{if } \; g_j(\boldsymbol{x}) \leq 0 \\ \rho_j = \text{a large positive number for all } j \text{ if } g_j(\boldsymbol{x}) > 0 \end{cases}$$

and β_k = a large positive number for all k.

For simplicity, the penalty parameters, ρ_j, j=1, 2, ..., m and β_k, k=1, 2, ..., r, take on the same positive value, ρ_j=β_k=μ. It can be shown that, as μ tends to infinity, the unconstrained minimum of $p(\boldsymbol{x})$ tends to the constrained minimum of the original problem defined by (4–6). In the application of the dynamic trajectory method used here and with the objective and gradient functions appropriately scaled, the penalty parameter μ is introduced at a certain specified value, here μ=10^2, and then increased to μ=10^4 when the intersection of active constraints is found. The dynamic trajectory method is applied to approximate sub-problems as follows.

Successive approximate quadratic sub-problems, $P[l]$; $l = 0, 1, 2, ...,$ are formed at successive design points $\boldsymbol{x}^{(l)}$, starting with an initial arbitrary design $\boldsymbol{x}^{(0)}$. Only the objective function approximation is explicitly discussed in what follows. Approximations $\tilde{g}_j(\boldsymbol{x})$ for the inequality constraints $g_j(\boldsymbol{x})$ and the approximations $\tilde{h}_k(\boldsymbol{x})$ to the equality constraint functions $h_k(\boldsymbol{x})$ may be obtained in a similar fashion. For

the sub-problem $P[l]$, the approximation $\tilde{f}(\boldsymbol{x})$ to $f(\boldsymbol{x})$ may be given by

$$\tilde{f}(\boldsymbol{x}) = f(\boldsymbol{x}^{(l)}) + \nabla^T f(\boldsymbol{x}^{(l)})(\boldsymbol{x} - \boldsymbol{x}^{(l)}) + \frac{1}{2}(\boldsymbol{x} - \boldsymbol{x}^{(l)})^T \mathbf{C}_j^{(l)} (\boldsymbol{x} - \boldsymbol{x}^{(l)}), \tag{8}$$

where $\nabla f(\boldsymbol{x})$ denotes the gradient vector. The approximate Hessian matrix ($\mathbf{C}_j^{(l)}$) is given by the diagonal matrix:

$$\mathbf{C}_j^{(l)} = \mathrm{diag}\left(c_j^{(l)}, c_j^{(l)}, \ldots, c_j^{(l)}\right) = c_j^{(l)}\mathbf{I}. \tag{9}$$

The initial values $c_j{}^{(0)}$ depend on the specific problem being considered. Here, a value of 0.0 was arbitrarily used for the first sub-problem (i.e. assuming a linear interpolation). Thereafter, the $c_j{}^{(l)}$ are calculated using the expression:

$$c_j^{(l)} = \frac{2\left\{f(\boldsymbol{x}^{(l-1)}) - f(\boldsymbol{x}^{(l)}) - \nabla^T f(\boldsymbol{x}^{(l)})(\boldsymbol{x}^{(l-1)} - \boldsymbol{x}^{(l)})\right\}}{\left\|\boldsymbol{x}^{(l-1)} - \boldsymbol{x}^{(l)}\right\|^2}, \tag{10}$$

where $\|\cdot\|$ denotes the Euclidian norm.

As a further aid in controlling convergence, intermediate move limits are imposed on the design variables during the minimisation of the sub-problem. These constraints are described by

$$\begin{aligned} x_i - x_i^{(l)} - \delta_i &\le 0 \\ -x_i + x_i^{(l)} - \delta_i &\le 0 \end{aligned} \quad ; \quad i = 1, 2, \ldots, n. \tag{11}$$

The approximate sub-problem $P[l]$ constructed at $\boldsymbol{x}^{(l)}$ is then

$$\text{Minimise } \tilde{f}(\boldsymbol{x}) \,, \quad \boldsymbol{x} \in R^n \tag{12}$$

subject to

$$\tilde{g}_j(\boldsymbol{x}) \le 0, \qquad j = 1, 2, ..., m$$

$$\tilde{h}_k(\boldsymbol{x}) = 0, \qquad k = 1, 2, ..., r.$$

Additional move limits (11) and side constraints are also prescribed. The optimum corresponding to the solution of $P[l]$ is denoted by $\boldsymbol{x}^{*(l)}$ with objective function value $f(\boldsymbol{x}^{*(l)})$. The starting point for the next sub-problem $P[l+1]$ is taken as $\boldsymbol{x}^{(l+1)}=\boldsymbol{x}^{*(l)}$.

The components of the gradient vector of the objective function in (8) at a specific design point $\boldsymbol{x}$, with respect to each of the design variables x_i, and used in the construction of the sub-problem are approximated by the first-order forward differencing scheme:

$$\frac{\partial f(\boldsymbol{x})}{\partial x_i} \approx \frac{f(\boldsymbol{x} + \Delta x_i) - f(\boldsymbol{x})}{\Delta x_i}; \; i = 1, 2, \ldots, n, \tag{13}$$

where $\Delta x_i=[0, 0, ..., \Delta x_i, ..., 0]^T$, and Δx_i is a suitable step size usually determined from a sensitivity study. It is clear that $n+1$ numerical analyses are required at each design point $\boldsymbol{x}$ to determine all the components of the constraint gradient vectors. The successive simple quadratic sub-problems are solved economically using the latest version of the trajectory method detailed by Snyman (1992).

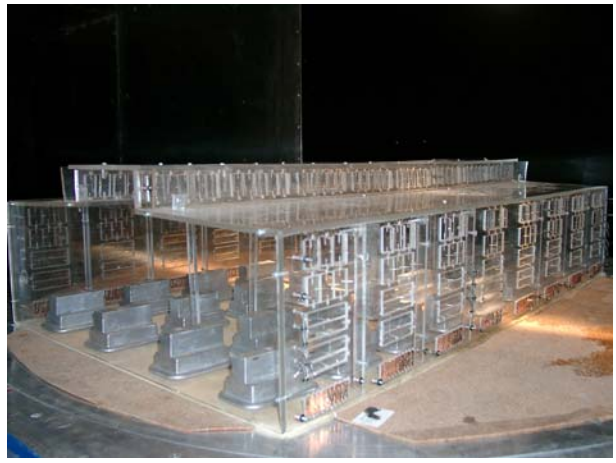

Fig. 2 The plexi-glass 1:80 scale model of the workshop on a rotary table in the wind tunnel

4 CFD modelling

Computational fluid dynamics simulations are computationally expensive because of the complexity and iterative nature of the numerical methods used to compute the flow patterns.The specific numerical method used to handle the problems in this study is the finite volume method, as implemented in the FLUENT software package (Fluent Inc. 2001). Even in the case of very fast computers, the computational time required for a full three-dimensional (3D) simulation using FLUENT may still be excessive when, to ensure convergence to a sufficiently accurate solution, a minimum number of computational iterations must be performed. Thus, the associated excessive computational time may exclude the possibility of performing a sufficient large number of simulations in attempting to obtain an optimum system. Of course, a two-dimensional (2D) model will require much less computational time per simulation than the 3D one. This is indeed the case here, where it has been found that a 3D analysis

Fig. 3 Visualization of the air inflow

Fig. 4 Flow-field visualization in a cross-section of the workshop

Table 1 Geometrical specifications of pot room

Size	
Height of the workshop, H (m)	17.12
Height of the CD	10H
Width of the workshop, W (m)	40.8
Width of the CD	10W
Number of smelter pots	4
Number of windows	
Bottom window (with fixed cross-section) on the left/right side of the hall	1/1
Middle window (with variable cross-section) on the left/right side of the hall	2/2
Roof window (with fixed cross-section) on the left/right side of the hall	1/1

CD Computational domain

(requiring 150 min per simulation) takes 25 times as long as a 2D analysis (6 min) for the same number (400) of iterations. It is therefore evident that, in this explorative investigation into the feasibility of optimising a system using formal mathematical optimisation, it is advisable to restrict the study to the use of a 2D model if it is sufficiently representative. Once the feasibility, and in particular the economy, of the optimisation approach as applied to the 2D case has been proven, one may, if necessary, proceed with relative confidence to its application to the more general and realistic 3D case.

4.1 Experimental and computational validation of numerical models

A very important consideration, before continuing to the numerical optimisation, is the validity of the numerical models to be used in the optimisation. This must be done from a physical experimental, as well as a computational, point of view. Although, to reduce the computational cost, it is preferable to use a 2D model in the final optimisation, it must first be validated against the more reliable 3D model. The particular 3D computational model used here is that detailed by Szabó et al. (2003), which was specifically developed for simulating the flow field inside the workshop. This 3D model was also used to obtain a reliable feel for the sensitivity of the air flow in the workshop to ambient parameters, such as temperature and wind velocity, and to adjustable physical settings, such as window angles.

The 3D numerical model was qualitatively and quantitatively validated via physical simulation using a scale model and by means of on-site measurements. The free parameters of the model were validated by local measurements using a 1:80 scale model in a wind tunnel, as summarized by Szabó (2003) and Szabó et al. (2005). Figure 2 shows the plexi-glass model in the wind tunnel. In these investigations, oil fog was used for visualization (see Figs. 3 and 4).

Further quantitative validation was done by means of on-site measurements of the mass flow rate of the workshop to determine the actual number of air changes per hour. This was done for the following representative weather conditions: ambient temperature, t_{amb}=7.9°C; velocity magnitude and direction of wind, v_0=1.2 m/s, northwest; and at a height of z_0=1.5 m. The wind direction was perpendicular to the sides of the workshop, i.e. perpendicular to the length axis of the workshop. The opening angle of the middle windows on the windward side was 30°, and at the leeward side, 40°. The velocities of the exiting air were measured at the roof windows at a few hundred different points. From these measurements, it was possible to determine the number of air changes of the workshop as L_{meas}=28.0/h. For the same conditions, the 3D simulation yielded the numerical solution $L_{num\ (3D)}$=26.5/h, which is in remarkable agreement (difference less than 5%), considering possible experimental errors in measurement and the existence of other peripheral and secondary factors, such as other buildings in the neighbourhood of the workshop, not taken into consideration in the numerical model. Further details regarding the comparison between measured and computed ventilation results are given by Szabó et al. (2005).

The above validation established confidence in the 3D model and allowed for its use in investigating the influence of various parameters and settings on the air flow patterns. In particular, these control investigations (Szabó 2004) were made by using the 3D numerical model and showed that the number of air changes per hour for fixed, half-range (partially) opened windows:

- Was independent of the ambient temperature.
- Was heavily dependent on the wind direction.
- Decreased slightly with increase in the wind profile exhibitor (explained below).

Table 2 Simulation settings (in FLUENT)

Heat flux through pots (W/m^2)	2,000
Turbulence model	Standard $k-\varepsilon$
Material	Air, with ideal gas law

Table 3 The boundary conditions and initial settings of the optimisation

Reference velocities, v_{ref} (m/s)	0	0.5	0.75	0.9	0.95	1	1.1	1.2	1.5	2	3	4	6	8
Ambient temperature (K)	300													
Initial values of design variables, x_1, ..., x_4	45°, 45°, −45°, −45° (measured clockwise from vertical)													

- Was dependent on the wind velocity if the reference speed is higher than 3 m/s.

Numerical simulations also showed that the ventilation number depends significantly on the opening angles of the windows. Furthermore, poor settings of the window angles may result in very strong blast occurring with the main part of the air mass being exhausted through the side windows and not through the roof windows as is preferred. In particular, the study showed that, in general, it is very difficult to predict what the appropriate window angles should be for a specific prevailing wind velocity. This preliminary 3D investigation thus justifies the choice of window angles as optimisation variables, which are to be adjusted to obtain optimal ventilation.

Finally, to justify the use of the computationally more economic 2D model in the place of the 3D model, its accuracy compared to that of the reliable 3D model has to be demonstrated. This was done by performing the 2D simulation for the same representative weather conditions, as that used in the validation of the 3D model above. For these conditions, the 2D simulation yields the number of air changes as $L_{\text{num (2D)}}$=25.0/h, compared to $L_{\text{num (3D)}}$=26.5/h for the 3D simulation. The agreement is very good, with the 2D value less than 6% lower than that for the 3D case. Moreover, since the 2D simulation gives a slightly lower value, the 2D model may be used with confidence in the optimisation, where the objective is to match the ideal minimum value of L_0=30/h. Thus, if the computed optimum solution corresponds to this value, one may expect that in the reality, the optimum values for the window angles will, at the very least, meet the minimum requirement.

4.2 The two-dimensional model for the optimisation

The main characteristic features of the 2D numerical model are now summarized. The velocity profile, also applied by Plate (1995), is determined by the following expression for atmospheric boundary layer flow:

$$v = v_{\text{ref}} \left(\frac{y}{y_{\text{ref}}} \right)^{\kappa}, \tag{14}$$

where y is the height above the ground, v_{ref} is a measured reference velocity and y_{ref} is the height of the measurement. Thus, the wind speed varies with distance (y) from the ground. As can be seen in this equation, the velocity distribution on a vertical plane has a power-law form. The shape of the velocity profile depends on the roughness of the ground surface. In (14), this roughness is taken into consideration by the characteristic exponent κ similar to Davenport (1982). In this study the modelling is performed with y_{ref}=1.5 m and κ=0.28. Further geometrical details of the model are as summarized in Table 1 (also refer to Fig. 1). The boundary condition and simulation settings are listed in Table 2.

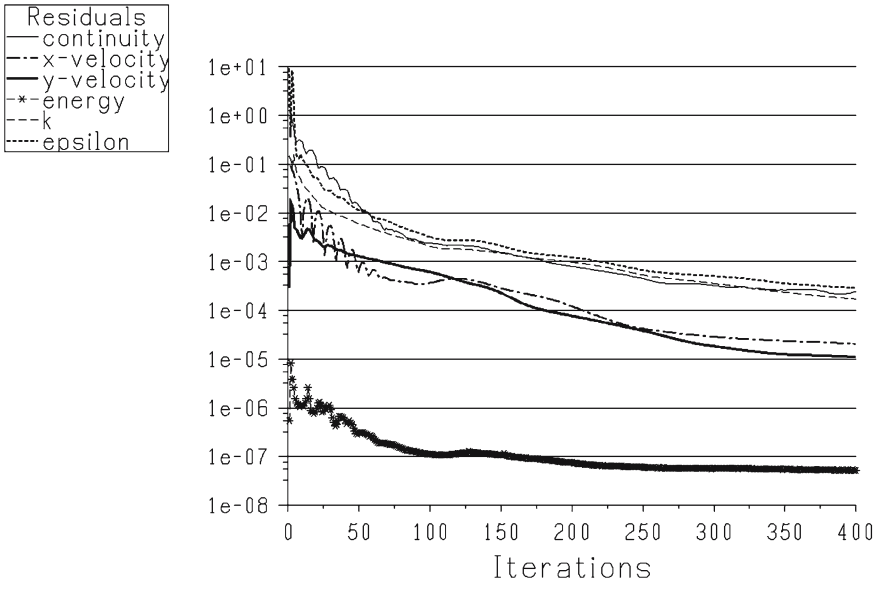

Fig. 5 Convergence of residuals in the case v_{ref}=4 m/s

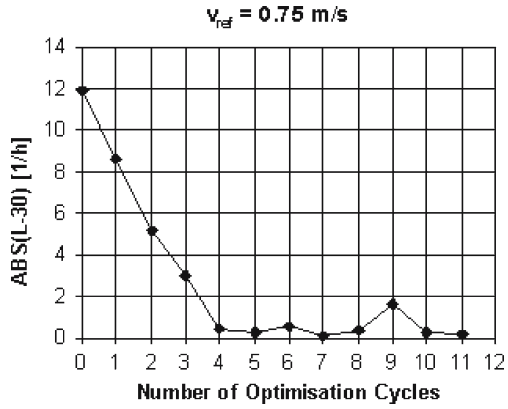

Fig. 6 Convergence history of objective function at v_{ref}=0.75 m/s

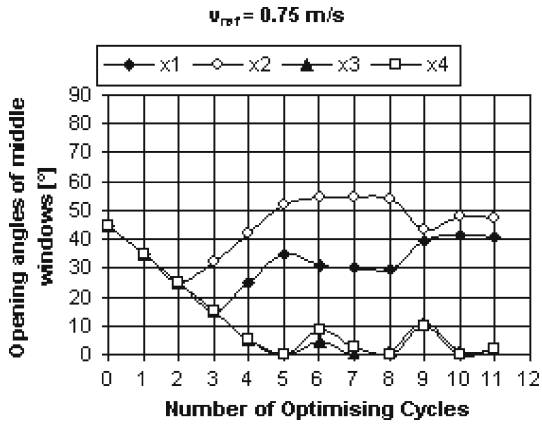

Fig. 7 Convergence histories of the design variables at v_{ref}=0.75 m/s

The smelter pots were modelled as heated walls, with prescribed heat flux. The value of 2,000 W/m^2 was computed from the energy consumption obtained from the plant data. One smelter pot requires 341 kW. The energy loss is about 170 kW. The swept surface of the pot is 85 m^2, giving a heat flux equal to 170,000/85≈2,000 W/m^2.

5 Numerical optimisation

5.1 Objective function

The objective function for the CFD optimisation is

$$f(\boldsymbol{x}) = |L(\boldsymbol{x}) - L_0|. \tag{15}$$

The design variables, adjusted in the optimisation, are the respective window angles x_1, x_2, x_3, x_4 (see Fig. 1). The optimisation procedure searches for the minimum of the objective function value (15), which corresponds to the best possible match between actual and prescribed number of air changes per hour. The optimisation is carried out for different prevailing wind velocities, corresponding to different weather conditions.

For the implementation of the Dynamic-Q algorithm, a *move limit* and a *forward finite difference step size* (for calculating approximations of the components of the gradient vector of the objective function) must be specified. The move limit specifies the maximum allowable jump that each variable may make per optimisation iteration or cycle. In this study, a move limit of 10° per variable was used, and a finite difference step size of 5° was used for computing the gradient component.

5.2 Numerical results

Results of the application of the numerical optimisation approach, detailed above, to an example problem are now presented. In this study, the effect of different wind velocities, corresponding to different weather conditions, is taken into account by considering 14 different reference wind velocity magnitudes.

Table 4 The optimum final value of the design variables x_1,..., x_4

Reference velocity, v_{ref} (m/s)	Number of optimisation cycles	Number of air changes L (1/h)	x_1 (°)	x_2 (°)	x_3 (°)	x_4 (°)
0	13	31.1	0	10	0	10
0.5	10	28.9	0	25	0	17
0.75	7	30.1	30	54	0	3
0.90	24	30.0	78	73	58	0
0.95	21	24.2	79	77	56	0
1.0	17	24.6	85	77	50	0
1.1	9	24.6	81	82	48	23
1.2	7	26.3	83	80	42	40
1.5	5	30.0	58	60	41	47
2.0	8	30.0	42	43	53	75
3.0	8	30.0	22	23	68	86
4.0	12	33.3	3	2	90	77
6.0	9	47.0	0	0	90	87
8.0	11	61.6	0	0	90	68

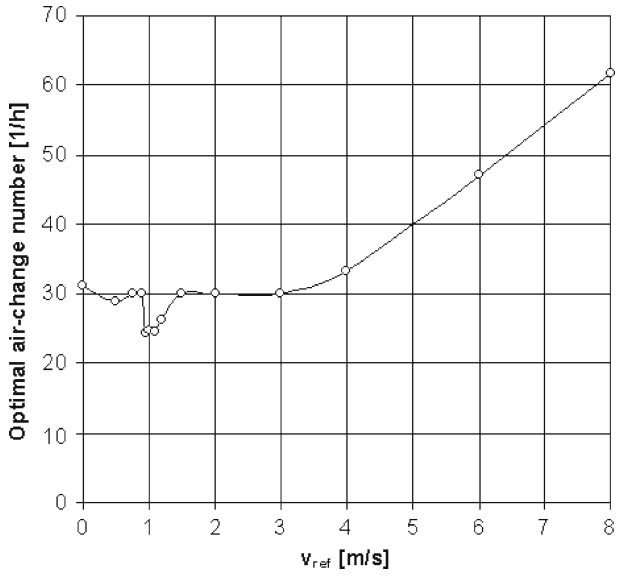

Fig. 8 The optimum number of air changes per hour

For each choice of wind velocity, the optimisation seeks the set of design variables (opening angles of windows), for which the number of air changes per hour is as close as possible to the prescribed or specified number, which for this example is taken to be L_0=30/h. Table 3 shows the reference speeds, the ambient temperature and the initial values of the design variables used.

CFD numerical simulations were performed using the default, built-in (predefined) features of the FLUENT software package. The standard $k-\varepsilon$ model for turbulence modelling was employed. The solver scheme was based on the first-order upwind differencing method. For the 2D geometry, the solver shows good convergence within 400 iterations (see Fig. 5). The run-time for 400 iterations of the FLUENT solver with up to 50,000 cells, for one set of window vane angles, takes approximately 6 min on a PIV 3 GHz computer. Thus, a whole optimisation process, with the solution of up to 20 sub-problems or cycles (see Section 3 above and numbers of cycles listed in Table 4), takes about 10 h to complete.

Typical of the results obtained is that for the case v_{ref}=0.75 m/s and presented graphically in Figs. 6 and 7. The very fast convergence of the objective function within five cycles, from a value of 12 to effectively 0, is evident from Fig. 6. Of particular interest is the fact that the algorithm apparently picks up more than one equivalent global minimum. The first strong local minimum corresponding to $\boldsymbol{x}^{(7)}$=[29.9, 54.5, 0.0, 2.7] with $f(\boldsymbol{x}^{(7)})$=0.05 is reached in the seventh cycle step. After a sharp jump at cycle 9, a second distinct and almost equivalent minimum is reached at cycle 11 with an $\boldsymbol{x}^{(11)}$=[40.7, 47.2, 1.9, 2.2] and $f(\boldsymbol{x}^{(11)})$=0.17. Both designs are acceptable. Note that $\boldsymbol{x}^{(l)}=\boldsymbol{x}^{*(l-1)}$, the optimum solution of the previous sub-problem.

The results for the other wind velocities are similar, also exhibiting the existence of multiple local minima. The distinct local minima for some of the other cases are listed below. In the case of v_{ref}=1.5 m/s, the following local minima are found:

$\boldsymbol{x}^{(5)}$=[57.8, 59.5, 41.1, 46.9] with $f(\boldsymbol{x}^{(5)})$=0.01 (cycle 5)
$\boldsymbol{x}^{(9)}$=[63.5, 66.1, 37.2, 63.3] with $f(\boldsymbol{x}^{(9)})$=0.14 (cycle 9)

In the case of v_{ref}=2.0 m/s, the following local minima are found:

$\boldsymbol{x}^{(3)}$=[39.3, 40.3, 54.0, 54.6] with $f(\boldsymbol{x}^{(3)})$=0.05 (cycle 3)
$\boldsymbol{x}^{(8)}$=[41.5, 42.8, 53.2, 74.5] with $f(\boldsymbol{x}^{(8)})$=0.02 (cycle 8)
$\boldsymbol{x}^{(13)}$=[48.7, 52.0, 70.5, 90.0] with $f(\boldsymbol{x}^{(13)})$=0.20 (cycle 13)

In the case of v_{ref}=3.0 m/s, the following local minima are found:

$\boldsymbol{x}^{(8)}$=[22.4, 22.6, 67.7, 86.1] with $f(\boldsymbol{x}^{(8)})$=0.01 (cycle 8)
$\boldsymbol{x}^{(13)}$=[23.0, 23.4, 74.0, 75.8] with $f(\boldsymbol{x}^{(13)})$=0.01 (cycle 13)
$\boldsymbol{x}^{(18)}$=[22.7, 24.0, 82.1, 85.9] with $f(\boldsymbol{x}^{(18)})$=0.16 (cycle 18)

By comparing the respective $\boldsymbol{x}$ components, it is clear that the optima listed are distinct from each other, yet they give effectively identical objective function values and are therefore equivalent.

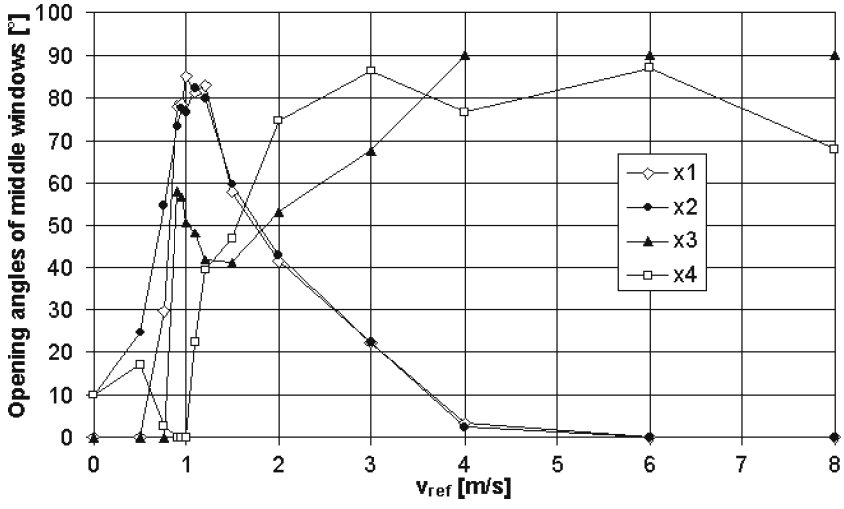

Fig. 9 The optimal angle of windows according to the reference velocity

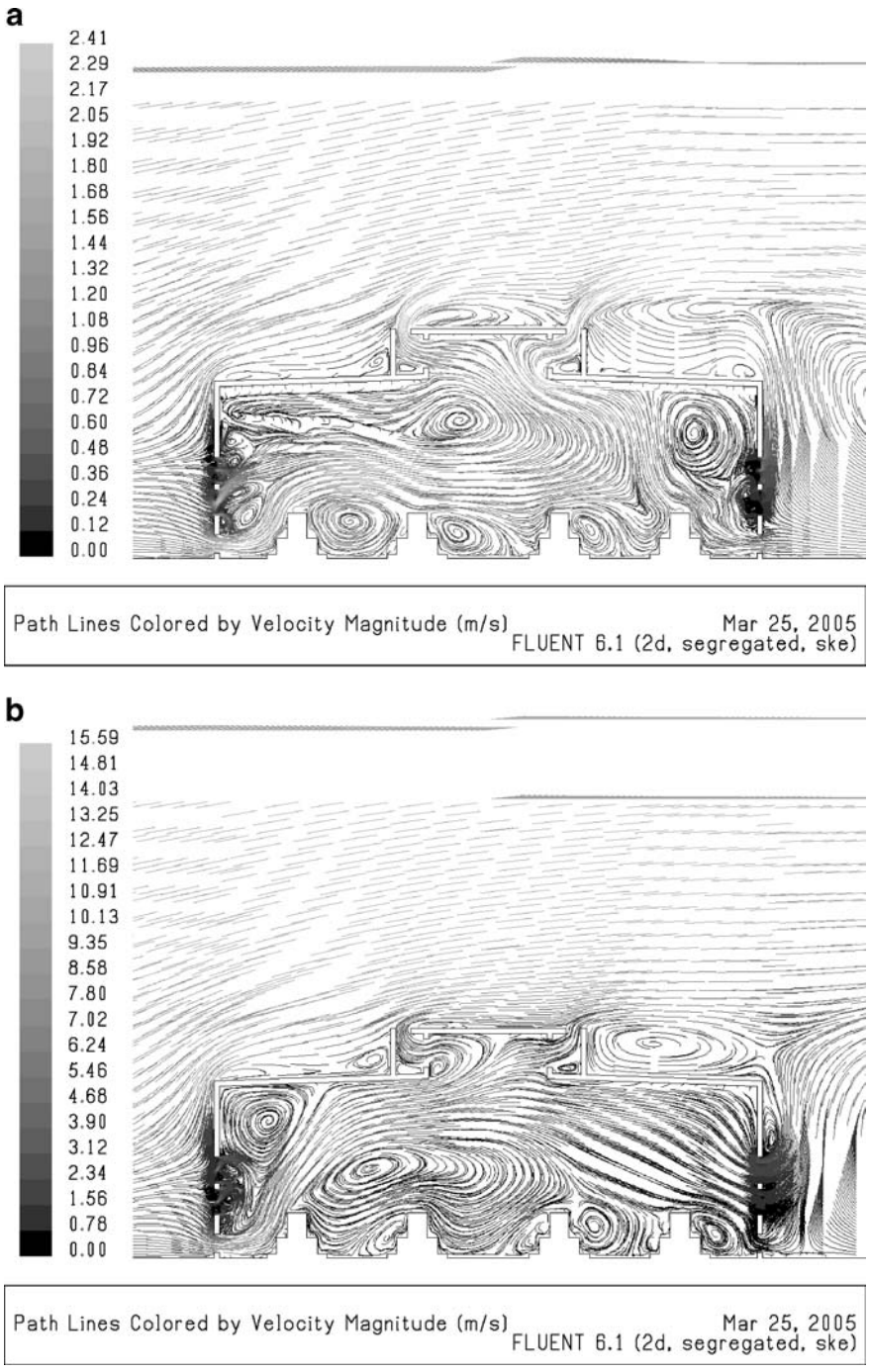

Fig. 10 Velocity, temperature and pressure field in and around the workshop are shown for two representative reference velocities (v_{ref}=0.5 m/s (c, a, e) and v_{ref}=4 m/s (b, d, f))

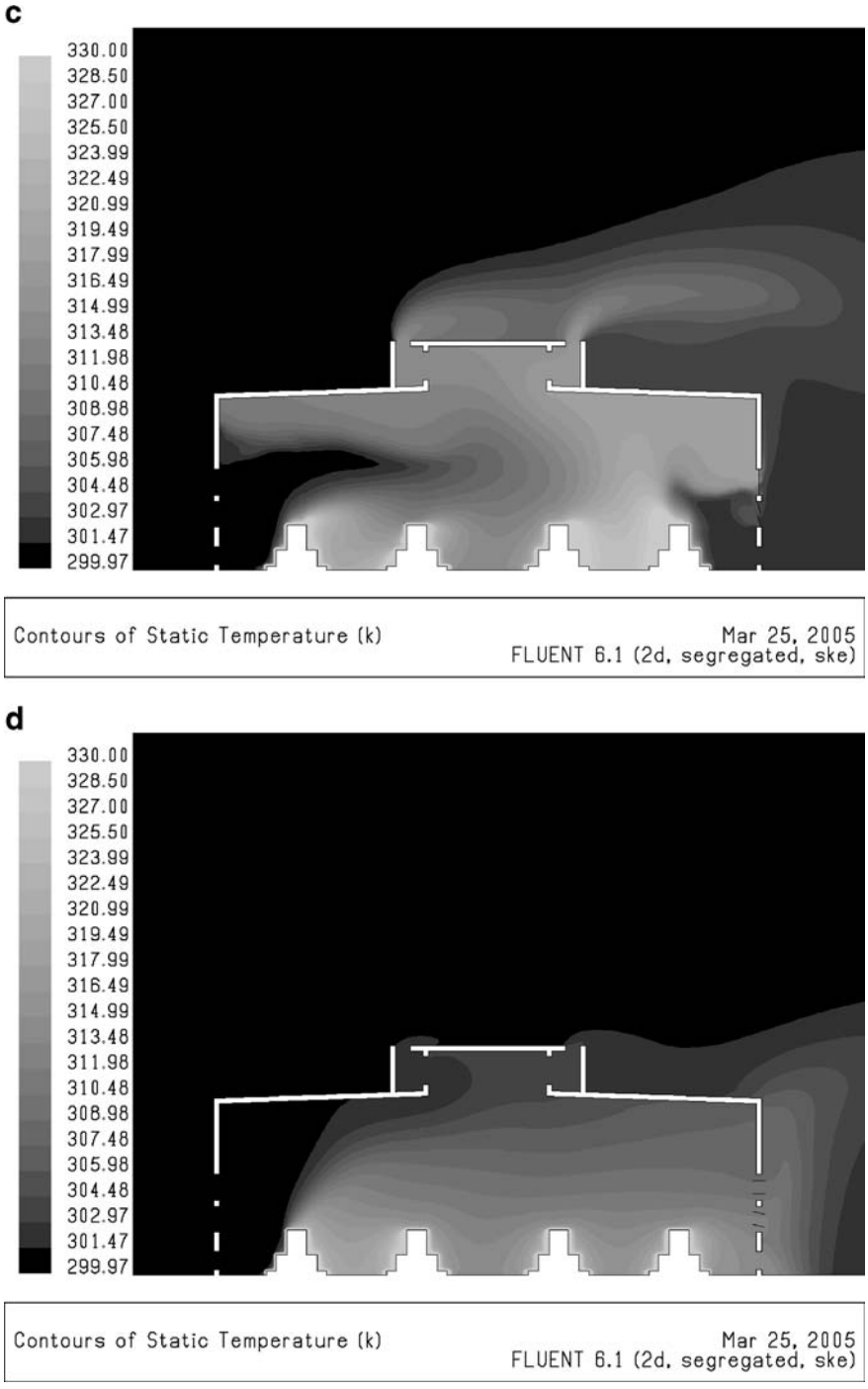

Fig. 10 (Continued)

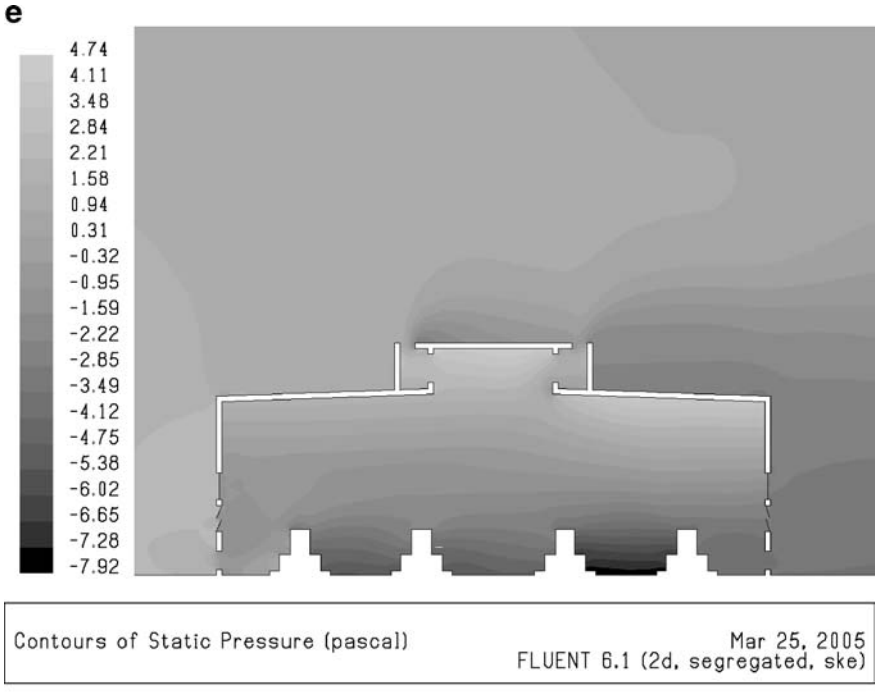

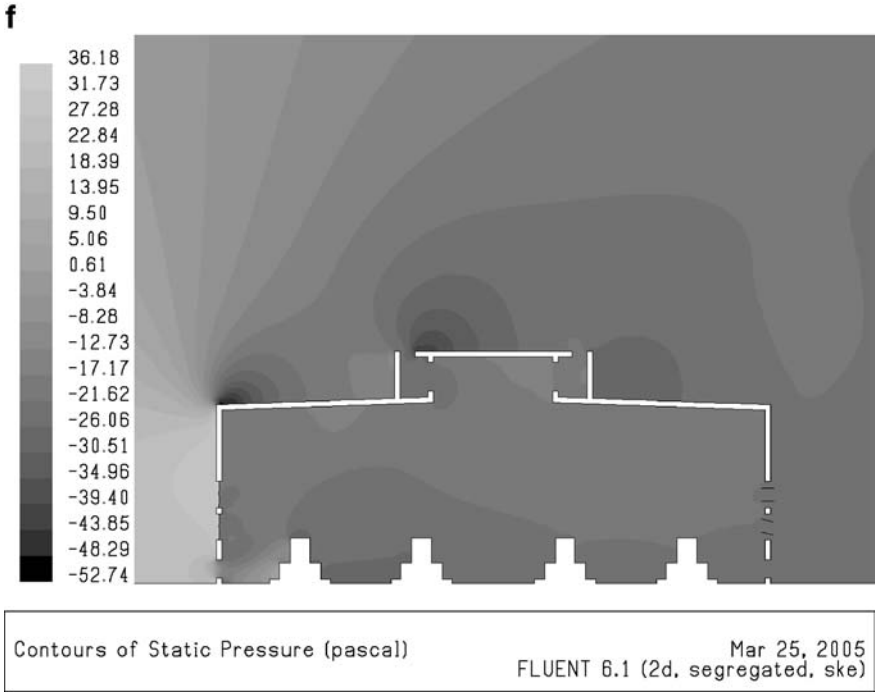

Fig. 10 (Continued)

The results for all of the wind velocity cases are summarized in Table 4 (listing only the result for the "best" global minimum where multiple minima exist) and in Figs. 8 and 9. Table 4 and Fig. 8 show that for reference velocities v_{ref}=1.5 to 3 m/s, the adjustment of the window angles to optimal values results in several air changes L that ideally match the prescribed value of L_0=30/h, giving an objective function value effectively equal to 0. At lower wind speeds, the nature of the air flow is very different because natural convection is dominant, and therefore, their results differ accordingly. In the case of v_{ref}=1 m/s, the number of air changes is less than that prescribed, in fact less than 20% of that required. Interesting is the fact that if no wind is present, the requirement of L=L_0=30/h is almost satisfied. Indeed, it is almost satisfied for a wide range of window angles. This is so because at zero wind velocity, the objective function is relatively insensitive to the design variables, with no real distinct local minimum occurring. For v_{ref}=0 m/s, the window angles for the best value of L=31/h, reached after 13 cycles, are listed in Table 4. Also for v_{ref}=0.5 m/s, the number of prescribed air changes are nearly met with L=28.9/h. In the case of high velocities ($v_{ref} > 3$ m/s), the side wind is so strong that the actual number of air changes cannot be reduced to the prescribed value, even if the middle windows are completely closed against the wind. The optimisation results obtained for these velocities represent the best solutions that can be achieved under these conditions. However, it should be noted that such strong winds are rarely encountered around the workshop. Moreover, the bottom windows can also be closed in the reality. In the case of extreme weather conditions they may be closed partially. Modelling their effect, however, introduces 3D aspects that cannot be modelled by the 2D model used here. Generally, the inner and outer pressure difference induces ventilation and air changes. If $v_{ref} > 3$ m/s, the forced convection becomes dominant, and the situation changes, with high pressure on the windward side and lower pressure on the leeward side.

The optimum middle window opening angles, listed in the last four columns of Table 4, are shown graphically in Fig. 9.

6 Discussion of results

With reference to Fig. 9, the following inferences may be made:

- The optimum opening angles of the two middle windows on, respectively the left side and the right, assume almost the same values, i.e. $x_1 \approx x_2$ and $x_3 \approx x_4$ for v_{ref} greater than 1 m/s.
- From the graphs in Fig. 9, it appears that the value v_{ref}=1 m/s corresponds to a special transitional case, since the tendencies of the results, above and below this value, clearly seem to switch. At this velocity, the windward middle windows (left side) are almost completely opened.
- If $v_{ref} > 1$ m/s, the left side middle windows should be closed gradually, and the others on the right side should be opened.
- If $v_{ref} > 4$ m/s, the windward middle windows are already totally closed, while the leeward ones on the right-hand side are almost totally opened. It appears that strong air blasts worsen the inner ventilation of the workshop.
- Moreover, if $v_{ref} > 4$ m/s, closing the middle windward windows completely is not sufficient to prevent an extremely high number of air changes occurring. In such cases, the partial closing of the bottom windows would be necessary. This case needs further investigation.

Figure 10 shows, for the optimal window settings, the characteristics of the air flow inside and around the workshop at two different representative reference wind velocities, namely, v_{ref}=0.5 m/s and v_{ref}=4 m/s. In the case of v_{ref}=0.5 m/s, a comparison of the cooling at the two different sides indicates the asymmetric nature of the cooling inside the workshop. In the case of v_{ref}=4 m/s, the fresh air enters the workshop only through the windward windows. The warmed-up and mixed air exits through both the roof and middle right windows. Although the high velocity results in effective cooling and lower pollutant concentration (due to dilution) within the workshop, the computed optimal behaviour does not allow the air to exit through the right middle windows. As a consequence, eddies evolve between the smelter pots, which are not physically acceptable and point to a failure of the 2D model used here. Since there are also corridors, running from left to right, between the rows of smelter pots in 3D space (see Fig. 2), there are other effects that, in reality, would prevent eddies' evolving. The pressure fields shown in Fig. 10 illustrate very clearly that the pent-up air on the windward side of the workshop causes significant pressure increases.

7 Conclusion

The study indicates that the proposed optimisation methodology can successfully be applied using the CFD simulation models. Optimal solutions with respect to appropriately chosen design variables that will ensure improved ventilation of a workshop for different weather conditions can be obtained. The deficiencies of the 2D model used here does not affect the general validity of the proposed optimisation methodology. Having proved the feasibility of the optimisation approach, further investigations in which it is planned to use a more realistic 3D CFD model may now be tackled with confidence. If this is done, the settings of the bottom windows (angle positions about vertical axes) may serve as additional design variables to be optimised in improving the ventilation. The unpleasant cross blasts of air may also be avoided by the specification of additional inequality constraints in the optimisation. This can be done with very little additional computational expense.

Acknowledgement The authors are grateful to OTKA (T 42781) for the financial support of this research. The study was also supported by the Hungarian–South African Intergovernmental S and T cooperation program DAK 7/2002. The Research and Technological Innovation Fund is the Hungarian partner, and the South African National Research Foundation is the South African partner.

References

Baturin WW (1959) Lüftungsanlagen für Indrustriebauten. VEB Verlag Technik, Berlin

Craig KJ, De Kock DJ, Snyman JA (1999) Using CFD and mathematical optimization to investigate air pollution due to stacks. Int J Numer Methods Eng 44:551–565

Davenport AG (1982) The interaction of wind and structures. In: Plate EJ (ed) Engineering meteorology. Elsevier, Amsterdam

Els PS, Uys PE (2003) Investigation of the applicability of the Dynamic-Q optimization algorithm to vehicle suspension design. Math Comput Model 37:1029–1046

Fluent Inc. (2001) Fluent Version 6 manuals. Fluent Inc., New Hampshire

Hay AM, Snyman JA (2005) Optimization of a planar tendon-driven manipulator for a maximal dextrous workspace. Eng Optim 37:217–236

Menyhárt J (1977) Handbook of building engineering. Mûszaki Könyvkiadó, Budapest (in Hungarian)

Plate E (1995) Windprobleme in dichtbesiedelten Gebieten. Windtechnologische Gesellschaft WTG, Karlsruhe (ISBN 3-928909-02-9)

Snyman JA (1982) A new dynamic method for unconstrained minimization. Appl Math Model 6:449–462

Snyman JA (1992) An improved version of the original leap-frog dynamic method for unconstrained minimization LFOP1(b). Appl Math Model 7:216–218

Snyman JA (2000) The LFOPC leap-frog algorithm for constrained optimisation. Comput Math Appl 40:1085–1096

Snyman JA (2005) Practical mathematical optimization—an introduction to basic optimization theory and classical and new gradient-based algorithms. Springer, Berlin, Heidelberg, New York, 257 pp (ISBN 0-387-24348-8)

Snyman JA, Hay AM (2002) The Dynamic-Q optimization method: an alternative to SQP? Comput Math Appl 44(14):1589–1598

Snyman JA, Frangos C, Yavin Y (1992) Penalty function solutions to optimal control problems with general constraints via a dynamic optimisation method. Comput Math Appl 23:46–47

Snyman JA, Stander N, Roux WJ (1994) A dynamic penalty function method for the solution of structural optimisation problems. Appl Math Model 18:453–460

Szabó Sz (2003) Intensification of natural and artificial aeration and minimization of emission in aluminium smelter-potrooms. Approaches to handling environmental problems in the mining and metallurgical regions. In: NATO Science Series. IV. Earth and Environmental Sciences, vol 20. Kluwer, Norwell, pp 197–209

Szabó Sz (2004) Numerical modelling the ventilation of a workshop by using the FLUENT commercial software package. Research final report, Miskolc, pp 1–46 (in Hungarian)

Szabó Sz, Schifter F (2000) Measuring and computing the natural ventilation of smelter pot room of the "Inotai Alumínium" Ltd. Research final report. Miskolc, pp 1–34 (in Hungarian)

Szabó Sz, Schifter F, Gyulai L, Lukács T, Szabó Á (2003) Modelling the natural ventilation of smelter potrooms. In: Proceedings of the conference on modelling fluid flow, Budapest, pp 660–667

Szabó Sz, Gyulai L, Tolvaj B (2005) Comparison of measured and computed ventilation of a workshop. *Gép* 56(8):49–54, (in Hungarian)

Visser JA, De Kock DJ (2002) Optimization of heat sink mass using the Dynamic-Q numerical optimization method. Commun Numer Methods Eng 18:721–727